

1 Tectonic settings of continental crust formation: Insights
2 from Pb isotopes in feldspar inclusions in zircon

3 **Hélène Delavault^{1,2}, Bruno Dhuime², Chris J. Hawkesworth^{1,2}, Peter A. Cawood¹,**
4 **Horst Marschall^{3,4}, and Edinburgh Ion Microprobe Facility (EIMF)⁵**

5 *¹Department of Earth Sciences, University of St. Andrews, North Street, St. Andrews*
6 *KY16 9AL, UK*

7 *²School of Earth Sciences, University of Bristol, Wills Memorial Building, Queens Road,*
8 *Bristol BS8 1RJ, UK*

9 *³Department of Geology and Geophysics, Woods Hole Oceanographic Institution, Woods*
10 *Hole, Massachusetts 02543, USA*

11 *⁴Goethe-Universität Frankfurt, Institut für Geowissenschaften, Altenhöferallee 1, 60438*
12 *Frankfurt am Main, Germany*

13 *⁵School of GeoSciences, University of Edinburgh, West Mains Road, Edinburgh EH9*
14 *3JW, UK*

15 **ABSTRACT**

16 Most crustal rocks derive from pre-existing crust, and so the composition of
17 newly generated (‘juvenile’) continental crust, and hence the tectonic settings of its
18 formation, have remained difficult to determine – especially over the first billion years of
19 Earth’s evolution. Modern primitive mantle-derived magmas have distinct U/Pb ratios,
20 depending on whether they are generated in intraplate (mean U/Pb = 0.37) or in
21 subduction settings (mean U/Pb = 0.10). The U/Pb ratio can therefore be used as a proxy
22 for the tectonic settings in which juvenile continental crust is generated. This paper

23 presents a new way to see back to the U/Pb ratios of juvenile continental crust that
24 formed 100's to 1000's of millions years ago, based on ion probe analysis of Pb isotopes
25 in alkali feldspar and plagioclase inclusions within well-dated zircons. Pb isotope data are
26 used to calculate the time-integrated U/Pb ratios (i.e., $^{238}\text{U}/^{204}\text{Pb} = \mu$) for the period
27 between the Hf model age and the U-Pb crystallization age of the zircons. These time-
28 integrated ratios reflect the composition of the juvenile continental crust at the time it was
29 extracted from the mantle, and so they can be used as a proxy for the tectonic setting of
30 formation of that crust. Two test samples with Proterozoic Hf model ages and Paleozoic
31 crystallization ages have feldspar inclusions with measured Pb isotope ratios that overlap
32 within analytical error for each sample. Sample Z7.3.1 from Antarctica has Pb isotope
33 ratios (mean $^{206}\text{Pb}/^{204}\text{Pb} = 16.88 \pm 0.08$, 1σ) that indicate it was derived from source
34 rocks with low U/Pb ratios (~ 0.11), similar to those found in subduction-related settings.
35 Sample TEMORA 2 from Australia has more radiogenic Pb isotope ratios (mean
36 $^{206}\text{Pb}/^{204}\text{Pb} = 19.11 \pm 0.23$, 1σ) indicative of a source with higher U/Pb ratios (~ 0.36),
37 similar to magmas generated in intraplate settings. Analysis of detrital populations with a
38 range of Hf model ages (e.g., Hadean to Phanerozoic), and for which zircons and their
39 inclusions represent the only archive of their parent magmas, should ultimately open new
40 avenues to our understanding of the formation and the evolution of the continental crust
41 through time.

42 INTRODUCTION

43 The continental crust provides the principal record of the Earth's evolution during
44 the past 4.4 billion years. Despite recent advances in analytical techniques and the
45 explosion in the number of high quality analyses of rocks, minerals and sediments of

46 various ages and provenance, the question of how the continental crust formed and
47 evolved through time remains controversial. It is widely accepted that most of the rocks
48 of the continental crust (80%–90%) available for sampling were themselves derived from
49 pre-existing crustal rocks (e.g., Belousova et al., 2010; Roberts and Spencer, 2014). Thus
50 the key to understanding the early stages of evolution of the continental crust is to
51 interrogate the geochemical record of the ‘juvenile’ crust, i.e. at the time of its extraction
52 from the mantle.

53 Dhuime et al. (2015) recently used Sr isotopes in whole rocks with a range of Nd
54 model ages of crust formation to evaluate the time-integrated Rb/Sr and silica contents of
55 juvenile continental crust. This study goes one step further and introduces a new
56 geochemical tool to distinguish subduction and intraplate settings of juvenile continental
57 crust generation. Our approach is based on the calculation of the time-integrated U/Pb
58 ratios from Pb isotope analyses of feldspar inclusions within zircon. The U-Pb system is
59 used because (i) measured U/Pb ratios are different in subduction-related magmas, which
60 have mean U/Pb = 0.10, and in intraplate-related magmas that have higher ratios and a
61 mean U/Pb = 0.37 (Fig. 1); (ii) feldspar contains sufficient Pb (typically 40–100 ppm in
62 alkali feldspar, Doe and Tilling, 1967) for small inclusions (typically 30–40 μm) to yield
63 precise isotope ratios when measured *in situ* with an ion probe (Table DR1); (iii) feldspar
64 has low U/Pb ratios such that the measured Pb isotope ratios can be taken to be the same
65 as those at the time of crystallization (Doe and Tilling, 1967; Doe et al., 1965); and (iv)
66 the time-integrated U/Pb ratio ($\mu = {}^{238}\text{U}/{}^{204}\text{Pb}$) can be determined from both ${}^{206}\text{Pb}/{}^{204}\text{Pb}$
67 and ${}^{207}\text{Pb}/{}^{204}\text{Pb}$ ratios (e.g., Oversby, 1974). Which of these two ratios is used depends on
68 the geological age, given the change from relatively more rapid ${}^{207}\text{Pb}$ ingrowth in the

69 Hadean and early Archean to more rapid ^{206}Pb ingrowth subsequently (e.g., Oversby,
70 1974; Stacey and Kramers, 1974).

71 Zircons preserve robust crystallization ages and their initial Hf isotope ratios
72 constrain when juvenile magma was separated from ambient mantle. This time is
73 commonly referred to as the Hf ‘model age’, because it is model-dependent (see a recent
74 review in Vervoort and Kemp, 2016). Inclusions in zircon occur in rocks of all ages and
75 provenance (Cavosie et al., 2004; Darling et al., 2009; Hopkins et al., 2008; Maas et al.,
76 1992; Nutman and Hiess, 2009), and inclusions such as apatite and biotite preserve trace
77 element contents that can be linked to those in the matrix, and those of the rocks from
78 which zircons crystallized (Jennings et al., 2011; Bruand et al., 2016). Radiogenic isotope
79 analyses in zircon and its mineral inclusions are now used here to explore the history of
80 the source precursor of these rocks. Integration of both trace element and isotope data on
81 mineral inclusions in the detrital zircon record will provide further insight into the
82 complex history of crustal evolution, especially for the early Earth where the rock record
83 is largely missing.

84 **SAMPLES AND METHODOLOGY**

85 This study was undertaken using two test samples, selected for a) the availability
86 of suitable material in Bristol; b) the presence of a few large (>30–40 μm) feldspar
87 inclusions within zircons (Figure S1 in the GSA Data Repository¹); and c) a time period
88 greater than 500 m.y. between the Hf model age and U-Pb crystallization age for each
89 sample, to ensure reasonable resolution for the calculation of time-integrated
90 parent/daughter trace element ratios in long-lived radioactive decay schemes (Dhuime et
91 al., 2015). Z7.3.1 is from a ca. 492 m.y. monzonite intrusion from Dronning Maud Land,

92 eastern Antarctica. The sample and the inclusions within zircons have been described by
93 Jennings et al. (2011), and zircons have a Paleoproterozoic (ca. 1.9 Ga) depleted mantle
94 Hf model age (Table DR2 in the GSA Data Repository¹). The second sample is the
95 TEMORA 2 zircon standard from the ca. 417 m.y. Middledale gabbroic diorite in the
96 Paleozoic Lachlan Orogen, eastern Australia (Black et al., 2004). It has a younger,
97 Meso/Neoproterozoic Hf model age of ca. 1.0 Ga (Table DR2 and Woodhead and Hergt
98 (2005)).

99 Heavy mineral fractions were concentrated using heavy liquids, and inclusion-rich
100 zircons were handpicked, mounted in epoxy, polished and examined by
101 cathodoluminescence, backscattered electron imaging, and energy-dispersive
102 spectrometry to identify and characterize feldspar inclusions. Pb isotope analyses on the
103 inclusions were carried out using a Cameca ims 1270 secondary ion mass spectrometer
104 (SIMS) at the Ion Microprobe Facility (EIMF), University of Edinburgh. Inclusions were
105 analyzed using a 4 nA O₂⁻ primary ion source with a 22 keV net impact energy. The beam
106 was focused using Köhler illumination to ensure a uniform beam density. The primary
107 beam alignment resulted in ellipsoidal analysis pits with a maximum major axis length of
108 ~15 µm. In order to limit peripheral contamination the spatial resolution of the analyzed
109 area was limited further by the use of a field aperture, which restricts the secondary ion
110 signal to the center of the analysis pit. A fixed 2700 µm field aperture was used
111 throughout and the blank was <0.003% of the signal measured on a zircon crystal. The
112 instrument was operated in 'rectangular mode' in order to maintain optimum conditions
113 for flat topped peaks. Pb isotopes were analyzed at a mass resolution of >4000R using a
114 peak switching routine. The BaSiO₂ peak was used for energy centering on each analysis

115 and a 100eV energy window was used throughout. The Zr₂O peak at mass 196 was used
116 to monitor potential overlap onto the zircon host. Secondary ion intensities were
117 measured using an electron multiplier in ion counting mode. A 5 μm² raster was applied
118 to the primary beam for 120 seconds in order to remove any surface contamination (e.g.,
119 ²⁰⁴Pb) around the sputter pit. Forty cycles of analysis were then made over the following
120 masses of interest; 196 (Zr₂O), 198(BaSiO₂), ²⁰⁴Pb, ²⁰⁶Pb, ²⁰⁷Pb, ²⁰⁸Pb. Each analysis
121 lasted 30 min in total. A mass fractionation correction of 2‰/amu was applied based on
122 previous measurements of natural glass and equal atom Pb standards. The repeat
123 measurements of ²⁰⁷Pb/²⁰⁶Pb and ²⁰⁸Pb/²⁰⁶Pb ratios of Shap Granite K-feldspar compared
124 to values of Tyrrell et al. (2006) similarly averaged 2‰/amu.

125 **RESULTS**

126 Pb isotope ratios were analyzed in feldspar inclusions in six zircons: four K-
127 feldspars and one plagioclase in sample Z7.3.1 (Antarctica), and two K-feldspars in
128 TEMORA 2 (Australia). One K-feldspar inclusion in zircon #75 from sample Z7.3.1 was
129 large enough to allow two analyses within the same inclusion (see light green triangles on
130 Figure 2 and SEM picture on Figure DR1 in the GSA Data Repository¹). All data are
131 plotted in Figure 2 with their associated analytical precision (2σ level), and reported in
132 Table DR1¹. SEM pictures of the analyzed samples, before and after SIMS analyses, are
133 provided in Figure DR1.

134 The feldspars in the two samples have very different Pb isotope ratios. K-
135 feldspars of sample Z7.3.1 (Antarctica) define a narrow range of Pb isotope compositions
136 with ²⁰⁶Pb/²⁰⁴Pb = 16.79–16.93, ²⁰⁷Pb/²⁰⁴Pb = 15.24–15.32 and ²⁰⁸Pb/²⁰⁴Pb = 36.36–
137 36.85, with 2 s.e. ~1.3% on average for these three isotope ratios (Table DR1). The

138 analysis of the single plagioclase inclusion is within error of those of the K-feldspar
139 inclusions (Fig. 2), but the uncertainty on Pb isotopes ratios for the plagioclase inclusion
140 is about twice as large as for K-feldspar (2 s.e._{plagioclase} ~2.8%), because of its lower lead
141 content (Doe and Tilling, 1967).

142 The abundance of K-feldspar inclusions within TEMORA 2 zircons is low, most
143 of the inclusions are very small (i.e., <<20 μm), and only two were large enough to be
144 analyzed (Fig. DR1). These inclusions have more radiogenic Pb isotope compositions
145 with $^{206}\text{Pb}/^{204}\text{Pb} = 19.27\text{--}19.95$, $^{207}\text{Pb}/^{204}\text{Pb} = 15.75\text{--}15.86$ and $^{208}\text{Pb}/^{204}\text{Pb} = 39.46\text{--}$
146 40.06 , with 2 s.e. errors of 1.3% (zircon #25) and 0.3% (zircon #27) on $^{206}\text{Pb}/^{204}\text{Pb}$.

147 **DISCUSSION**

148 **A 2-Stage Model to Calculate the U/Pb Ratio of the Juvenile Continental Crust**

149 Our approach uses a two-stage model to calculate the $\mu = ^{238}\text{U}/^{204}\text{Pb}$ ratio of the
150 juvenile continental crust (Fig. 3A). Stage 1 is the period of Pb isotope evolution of the
151 juvenile continental crust, from its extraction from a depleted mantle reservoir until the
152 formation of a derivative crustal melt from which the zircons and their inclusions
153 subsequently crystallized. Stage 2 is the period from the crystallization of those melts to
154 the present day. Our model therefore relies on knowing the crystallization age of the
155 zircon, and its model age that constrains when the source of the magma from which the
156 zircon crystallized was derived from the mantle. The measured Pb isotope ratios of the
157 feldspar inclusions are used to back-calculate the U/Pb ratios of the juvenile continental
158 crust (JCC) in the periods between the Hf model ages and the U-Pb crystallization age
159 (i.e., Stage 1), following Equations 1 and 2 below:

$$160 \quad (\mu)_{JCC} = \frac{\frac{^{206}\text{Pb}}{^{204}\text{Pb}}^{\text{Fsp}} - \frac{^{206}\text{Pb}}{^{204}\text{Pb}}^{\text{DM}}}{e^{(\lambda \times T_{\text{DM}})} - e^{(\lambda \times T_{\text{cryst zrn}})}} \quad (1)$$

161 Where $T_{\text{cryst zrn}}$ is the U-Pb crystallization age of the zircon, T_{DM} is the depleted
 162 mantle (DM) Hf model age of the zircon (calculated assuming a linear evolution of the
 163 DM from $\epsilon_{\text{Hf}} = 0$ at 4560 Ma to $\epsilon_{\text{Hf}} = 17$ at present, and an assumed $^{176}\text{Lu}/^{177}\text{Hf} = 0.015$
 164 for the crustal source from which the zircon crystallized), λ is the decay constant of ^{238}U
 165 ($1.55125 \times 10^{-10} \text{ y}^{-1}$), $(^{206}\text{Pb}/^{204}\text{Pb})^{\text{Fsp}}_{\text{meas}}$ is the measured $^{206}\text{Pb}/^{204}\text{Pb}$ ratio in the feldspar
 166 inclusion, and $(^{206}\text{Pb}/^{204}\text{Pb})^{\text{DM}}_{\text{at } T_{\text{DM}}}$ is the Pb isotope composition of the depleted mantle
 167 at T_{DM} . The Pb isotope evolution of the mantle was calculated using the composition of
 168 the Canyon Diablo troilite (CDT) at $t_0 = 4560$ Ma and a 2-stage model similar to that of
 169 Stacey and Kramers (1975), in which $\mu_{1(4560-3700\text{Ma})} = 7.13$ and $\mu_{2(3700-0\text{Ma})} = 9.33$ where
 170 chosen to match the Gale et al. (2013) present-day MORB average. This mantle Pb
 171 isotope evolution curve is similar to those previously published by Kramer and Tolstikhin
 172 (1997) and Kamber (2015).

$$173 \quad \left(\frac{\text{U}}{\text{Pb}}\right)_{JCC} = \frac{(\mu)_{JCC}}{\left(\frac{M_{\text{Pb}}}{M_{\text{U}}}\right) \times \left(\frac{\text{ab}^{238}\text{U}}{\text{ab}^{204}\text{Pb}}\right)} \quad (2)$$

174 Where M_{U} and M_{Pb} are the standard atomic weights of U and Pb, and ab^{238}U and
 175 ab^{204}Pb are the relative abundances of ^{238}U as percent of total U and ^{204}Pb as percent of
 176 total Pb, respectively.

177 In principle, our 2-stage model can also be applied to the $^{207}\text{Pb}/^{204}\text{Pb}$ isotopic
 178 system. However given that the half-life of the decay of ^{235}U to ^{207}Pb is ~6 times lower
 179 than that of ^{238}U to ^{206}Pb , the evaluation of $^{235}\text{U}/^{207}\text{Pb}$ with this method appears better
 180 suited to samples with Hadean/early Archean model ages.

181 **Application of the Method**

182 The Antarctica sample Z7.3.1 is particularly well suited for this study, because of
183 the presence of large and abundant K-feldspar inclusions within the zircons (see Fig.
184 DR1), and because there is ca. 1.4 billion years between its Hf model age and
185 crystallization age. This period is often referred to as the ‘residence time’, and it is long
186 enough to offer reasonable resolution on the back-calculation of the U/Pb ratios of the
187 juvenile continental crust ((U/Pb)_{JCC}). The (U/Pb)_{JCC} ratios calculated for five K-feldspar
188 inclusions in this sample range from 0.11 to 0.12 (Fig. 3B), and these ratios are similar to
189 the values observed in recent subduction-related magmas (see Fig. 1). Thus, although the
190 host monzonite magma for the zircons (and their inclusions) crystallized in the early
191 Paleozoic during the later stages of the collisional assembly of East and West Gondwana
192 (Jacobs and Thomas, 2004), the monzonite magma was derived from crust that originally
193 separated from the mantle around 1.9 billion years ago in a subduction-related
194 environment. Flowerdew et al. (2012) analyzed K-feldspar separates from two ca. 520
195 m.y. granitoids from Dronning Maud Land, and they reported ²⁰⁶Pb/²⁰⁴Pb ratios of 16.45–
196 16.54. Calculated (U/Pb)_{JCC} ratios for these feldspars (ca. 0.09) also fall in the range of
197 subduction-related magmas (Fig. 1), and so the tectonic setting of the continental crust
198 formation indicated by both feldspars from bulk rocks and from inclusions within zircons
199 is similar.

200 TEMORA 2 has a residence time of ca. 0.6 billion years that is also taken to be
201 large enough to estimate U/Pb ratios in its source (Fig. 3A). The results are presented in
202 Figure 3B, and the calculated (U/Pb)_{JCC} ratios range from 0.34 to 0.39. These ratios are
203 higher than the U/Pb ratios in most subduction-related magmas, but they are similar to

204 the U/Pb ratios in intraplate magmas (Fig. 1). We conclude that the crustal source of the
205 TEMORA magma was generated in an intraplate setting at ~1.0 Ga, consistent with
206 paleogeographic reconstructions that place eastern Australia adjacent to western
207 Laurentia within the Rodinian supercontinent (e.g., Hoffman, 1991).

208 **Implications of the New Method**

209 This study demonstrates that back-calculation of the U/Pb ratios of juvenile
210 continental crust can be used to constrain whether new crustal material was generated in a
211 subduction (Z7.3.1) or an intraplate (TEMORA 2) setting. Our approach highlights the
212 potential of interrogating the isotope record of mineral inclusions encapsulated within
213 zircons. Mineral inclusions offer a richer record of the evolution of the magmatic rocks
214 than does the mineral zircon, which tends to crystallize at a relatively late stage in the
215 evolution of the parent magma. Pb isotope analysis of feldspar inclusions within zircons
216 therefore represents a new addition to the geochemical toolbox for unraveling the
217 evolution of the continental crust through time. The use of this method on magmatic and
218 detrital zircons with a range of Hf model ages covering Earth's history from the Hadean
219 to Phanerozoic has the potential to open new avenues into our understanding of the large-
220 scale evolution of the continental crust.

221 **ACKNOWLEDGMENTS**

222 This work was supported by the Natural Environment Research Council (NERC
223 grants NE/J021822/1 and NE/K008862/1) and by the Leverhulme Trust (grant RPG-
224 2015-422). We thank S. Kearns and B. Buse for their technical assistance during SEM
225 imaging. Thorough and constructive comments from M. Whitehouse, J.B. Murphy and

226 two anonymous reviewers have been greatly appreciated during the preparation of this
227 article.

228 **REFERENCES CITED**

- 229 Belousova, E.A., Kostitsyn, Y.A., Griffin, W.L., Begg, G.C., O'Reilly, S.Y., and
230 Pearson, N.J., 2010, The growth of the continental crust: Constraints from zircon Hf-
231 isotope data: *Lithos*, v. 119, p. 457–466, doi:10.1016/j.lithos.2010.07.024.
- 232 Black, L.P., Kamo, S.L., Allen, C.M., Davis, D.W., Aleinikoff, J.N., Valley, J.W.,
233 Mundil, R., Campbell, I.H., Korsch, R.J., Williams, I.S., and Foudoulis, C., 2004,
234 Improved $^{206}\text{Pb}/^{238}\text{U}$ microprobe geochronology by the monitoring of a trace-
235 element-related matrix effect; SHRIMP, ID-TIMS, ELA-ICP-MS and oxygen
236 isotope documentation for a series of zircon standards: *Chemical Geology*, v. 205,
237 p. 115–140, doi:10.1016/j.chemgeo.2004.01.003.
- 238 Bruand, E., Storey, C.D, and Fowler, M.B., An apatite for progress: Inclusions in zircon
239 and titanite constrain petrogenesis and provenance: *Geology*, G37301.1, first
240 published on January 4, 2016, doi:10.1130/G37301.1.
- 241 Cavosie, A.J., Wilde, S.A., Liu, D., Weiblen, P.W., and Valley, J.W., 2004, Internal
242 zoning and U–Th–Pb chemistry of Jack Hills detrital zircons: a mineral record of
243 early Archean to Mesoproterozoic (4348–1576 Ma) magmatism: *Precambrian*
244 *Research*, v. 135, p. 251–279, doi:10.1016/j.precamres.2004.09.001.
- 245 Darling, J., Storey, C., and Hawkesworth, C., 2009, Impact melt sheet zircons and their
246 implications for the Hadean crust: *Geology*, v. 37, p. 927–930,
247 doi:10.1130/G30251A.1.

- 248 Dhuime, B., Wuestefeld, A., and Hawkesworth, C.J., 2015, Emergence of modern
249 continental crust about 3 billion years ago: *Nature Geoscience*, v. 8, p. 552–555,
250 doi:10.1038/ngeo2466.
- 251 Doe, B.R., and Tilling, R.I., 1967, The Distribution of lead between coexisting K-
252 feldspar and plagioclase: *The American Mineralogist*, v. 52, p. 805–816.
- 253 Doe, B.R., Tilton, G.R., and Hopson, C.A., 1965, Lead isotopes in feldspars from
254 selected granitic rocks associated with regional metamorphism: *Journal of*
255 *Geophysical Research*, v. 70, p. 1947–1968, doi:10.1029/JZ070i008p01947.
- 256 Flowerdew, M.J., Tyrrell, S., Riley, T.R., Whitehouse, M.J., Mulvaney, R., Leat, P.T.,
257 and Marschall, H.R., 2012, Distinguishing East and West Antarctic sediment sources
258 using the Pb isotope composition of detrital K-feldspar: *Chemical Geology* v. 292–
259 293, p. 88–102, doi: 10.1016/j.chemgeo.2011.11.006.
- 260 Gale, A., Dalton, C.A., Langmuir, C., Su, Y., and Shilling, J.-G., 2013, The mean
261 composition of ocean ridge basalts: *Geochemistry, Geophysics, Geosystems*, v. 14,
262 doi:10.1029/2012GC004334.
- 263 Hoffman, P.F., 1991, Did the Breakout of Laurentia Turn Gondwanaland Inside-Out?:
264 *Science*, v. 252, p. 1409–1412, doi:10.1126/science.252.5011.1409.
- 265 Hopkins, M., Harrison, T.M., and Manning, C.E., 2008, Low heat flow inferred from >4
266 Gyr zircons suggests Hadean plate boundary interactions: *Nature*, v. 456, p. 493–
267 496, doi:10.1038/nature07465.
- 268 Jacobs, J., and Thomas, R.J., 2004, Himalayan-type indenter-escape tectonics model for
269 the southern part of the late Neoproterozoic–early Paleozoic East African– Antarctic
270 orogen: *Geology*, v. 32, p. 721–724, doi:10.1130/G20516.1.

- 271 Jennings, E.S., Marschall, H.R., Hawkesworth, C.J., and Storey, C.D., 2011,
272 Characterization of magma from inclusions in zircon: Apatite and biotite work well,
273 feldspar less so: *Geology*, v. 39, p. 863–866, doi:10.1130/G32037.1.
- 274 Kamber, B.S., 2015, The evolving nature of terrestrial crust from the Hadean, through the
275 Archaean, into the Proterozoic: *Precambrian Research*, v. 258, p. 48–82,
276 doi:10.1016/j.precamres.2014.12.007.
- 277 Kramers, J.D., and Tolstikhin, I.N., 1997, Two terrestrial lead isotope paradoxes, forward
278 transport modelling, core formation and the history of the continental crust:
279 *Chemical Geology*, v. 139, p. 75–110, doi: 10.1016/S0009-2541(97)00027-2.
- 280 Maas, R., Kinny, P.D., Williams, I.S., Froude, D.O., and Compston, W., 1992, The
281 Earth's oldest known crust: A geochronological and geochemical study of 3900–
282 4200 Ma old detrital zircons from Mt. Narryer and Jack Hills, Western Australia:
283 *Geochimica et Cosmochimica Acta*, v. 56, p. 1281–1300, doi:10.1016/0016-
284 7037(92)90062-N.
- 285 Nutman, A.P., and Hiess, J., 2009, A granitic inclusion suite within igneous zircons from
286 a 3.81 Ga tonalite (W. Greenland): Restrictions for Hadean crustal evolution studies
287 using detrital zircons: *Chemical Geology*, v. 261, p. 77–82,
288 doi:10.1016/j.chemgeo.2008.09.005.
- 289 Oversby, V.M., 1974, New look at the lead isotope growth curve: *Nature*, v. 248, p. 132–
290 133, doi:10.1038/248132a0.
- 291 Roberts, N.M.W., and Spencer, C.J., 2014, The zircon archive of continent formation
292 through time: *Geological Society of London, Special Publications*, v. 389, p. 197–
293 225, doi:10.1144/SP389.14.

- 294 Stacey, J.S., and Kramer, J.D., 1975, Approximation of terrestrial lead isotope evolution
295 by a two-stage model: *Earth and Planetary Science Letters*, v. 26, p. 207–221,
296 doi:10.1016/0012-821X(75)90088-6.
- 297 Tyrrell, S., Haughton, P.D.W., Daly, J.S., Kokfelt, T.F., and Gagnevin, D., 2006, The use
298 of the common Pb isotope composition of detrital K-Feldspar grains as a provenance
299 tool and its application to upper Carboniferous paleodrainage, Northern England:
300 *Journal of Sedimentary Research*, v. 76, p. 324–345, doi:10.2110/jsr.2006.023.
- 301 Vervoort, J.D., and Kemp, A.I.S., 2016, Clarifying the zircon Hf isotope record of crust–
302 mantle evolution: *Chemical Geology*, v. 425, p. 65–75,
303 doi:10.1016/j.chemgeo.2016.01.023.
- 304 Woodhead, J.D., and Hergt, J.M., 2005, A Preliminary appraisal of seven natural zircon
305 reference materials for in situ Hf isotope determination: *Geostandards and*
306 *Geoanalytical Research*, v. 29, p. 183–195, doi:10.1111/j.1751-
307 908X.2005.tb00891.x.

308

309 **FIGURE CAPTIONS**

310

311 Figure 1. Present-day distribution of U/Pb ratios in mafic rocks (filled color histograms)
312 and olivine-hosted melt inclusions (hollow black histograms) in subduction and intraplate
313 (OIB) settings. Data are from the GEOROC database ([http://georoc.mpch-](http://georoc.mpch-mainz.gwdg.de/georoc/)
314 [mainz.gwdg.de/georoc/](http://georoc.mpch-mainz.gwdg.de/georoc/)), with analyses selected from primitive fresh basaltic whole rocks
315 (i.e. SiO₂ = 45–53%, MgO = 7–25%, LOI < 5% and sum of major elements > 95%) of
316 volcanic origin.

317

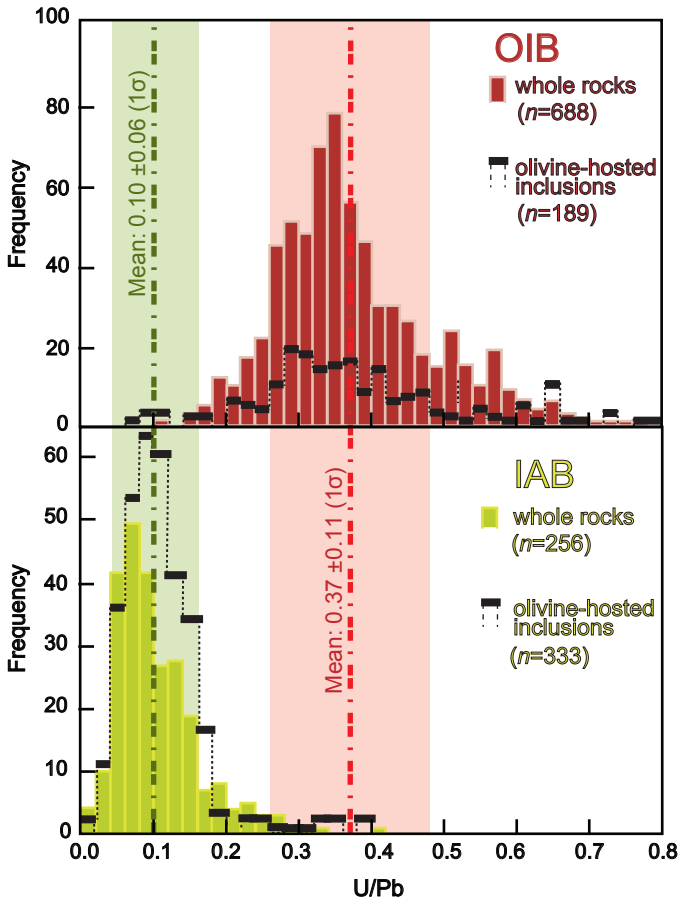
318 Figure 2. $^{207}\text{Pb}/^{204}\text{Pb}$ versus $^{206}\text{Pb}/^{204}\text{Pb}$ plot for mineral inclusions in sample Z7.3.1
319 (green) and TEMORA 2 (red) analyzed by SIMS. All but one (dark green square,
320 plagioclase) analyses were in K-feldspars. Light green triangles show two analyses within
321 a same inclusion in sample Z7.3.1 (zircon #75, see Figure DR1).

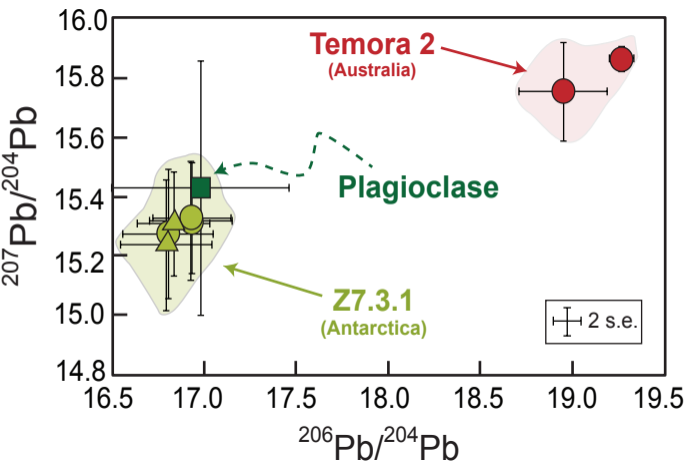
322

323 Figure 3. Evolution of the $^{206}\text{Pb}/^{204}\text{Pb}$ ratios through time. (A) Schematic representation
324 of the calculation of the ‘Stage 1’ time-integrated U/Pb of juvenile continental crust,
325 between the time of its separation from the depleted mantle (blue star) and the
326 crystallization of the zircon host of the feldspar (Fsp) inclusions (red and green dots).
327 Typical evolution paths for new crust generated in intraplate setting (red curve) and in
328 subduction setting (green curve) are presented. The depleted mantle evolution is the black
329 DM line. (B) Time-integrated U/Pb ratios calculated for two test samples Z7.3.1 (green
330 dots) and TEMORA 2 (red dots), from the combination of U-Pb and Hf data in zircon
331 and Pb isotope data in feldspar inclusions.

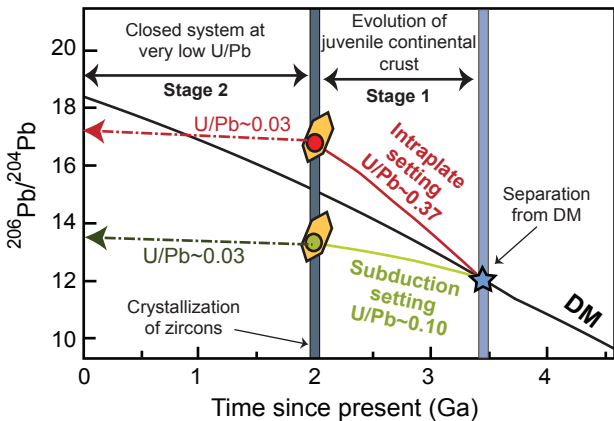
332

333 ¹GSA Data Repository item 201Xxxx, **Supplementary Figure DR1; Supplementary**
334 **methods and references**, is available online at www.geosociety.org/pubs/ft20XX.htm,
335 or on request from editing@geosociety.org.





(A) Method



(B) Application

